Compton Scattering

Gruppo n.12
Candiello Anita 1146534
Lonigro Nicola 1218058
Pergola Paolo 1238256

November 2019

Objectives

- Verify the relationship between energy and angle of the diffused photon in a Compton scattering.
- Measure the differential cross section of Compton scattering

DUE TO PROBLEM WITH THE PORT OF THE DIGITIZER AND THE VERDI SOFTWARE, NO DATA WAS TAKEN WITH THE DIGITIZER ON THE FIRST DAY, SO IT WAS NOT POSSIBLE TO COMPLETE ALL THE OBJECTIVES AS SCHEDULED FOR THE EXPERIMENT.

Materials and Instrumentations

- 2 Na-22 sources
- Am-241 source
- 3 NaI(Tl) scintillator detectors (TAGGER, SCATTERER, DETECTOR)
- CAEN N8315 power module
- CAEN digitizer DT5720
- 3 CFTD mod. INFN Pd
- SEN mod. LU 278
- Phillips Scientific model 744 Quad linear gate Fan-in/out
- CAEN mod. N145 Quad Scaler and Preset Counter Timer
- Tektronix TDS 1012B Oscilloscope

Calibration of the detectors

The intensity of the signals coming out of the detectors corresponding to the 511 keV photon from electron positron-annihilation and the 1275 keV photon from the Na-22 source were measured with the oscilloscope, giving the results in Tab.1. The measured rise times, fall times, noise levels and rates measured with the oscilloscope are also reported.

After adjusting the thresholds to cut off the noise from the electronics the spectra of the detectors were acquired, one at a time, by sending the signal through the CFTD and then to the digitizer. An additional peak was obtained by acquiring the spectrum of an Am-241 source, with its characteristic 59 keV peak, with each scintillator. The 3 peaks were fitted by a gaussian and the resulting three points were fitted with a line (Fig.1) to obtain the relation between channels and energies.

The fraction of events in the full-energy peak of the 511 keV photon with respect to the total number of events of the TAGGER was estimated by dividing the number of events with an energy lower than the 564 keV (the energy of the photon plus three times the sigma of the peak fit) by the total number of events after removing the expected compton background from the 1275 keV peak. The factor F(511) obtained is equal to 0.4891 ± 0.0007.

To evaluate the relation between the number of events and the error on the determination of the centroid of the peak, multiple measurement of the DETECTOR Na-22 spectrum were taken with an increasingly higher number of events. In Fig.2 the error on the position as a function of the area under the peak is plotted, showing the expected $\frac{1}{\sqrt{N}}$ relation.

Measurements of the energy of scattered photons

In order to verify the following theoretical relationship between the energy of the 511 keV emitted photon and the angle of scattering:

$$h\nu_f = \frac{h\nu_i}{1 + \frac{h\nu_i}{m_e c^2}(1 - cos\theta)} \tag{1}$$

where m_e is the electron mass and c is the velocity of light, the photon which hits the SCATTERER was selected with the use of the TAGGER, considering the coincidence with a second 511 keV photon emitted by the source. This coincidence is used to provide the trigger for the scattered event and to normalize the measurements revealed by the DETECTOR. The three outputs of the detectors were connected to a Quad Linear Gate FAN-IN/OUT for signal doubling: a signal was inserted directly in the CAEN digitizer while the second one was connected to the input of one of the CFTD. In order to create a coincidence between the output signals, a region of overlapping for the CFTDs'

Photon energy (keV)	**V (mV)**	**Fall Time (ns)**	**Rise Time (ns)**	**Noise Level (mV)**
TAGGER				
511	61.1 ± 3	33.60 ± 6	425.6 ± 6	66 ± 3
1275	142 ± 5	43.60 ± 6	498.2 ± 6	66 ± 3
SCATTERER				
511	60.0 ± 3	28.45 ± 6	391.2 ± 6	62 ± 3
1275	139 ± 6	48.20 ± 6	475.3 ± 6	62 ± 3
DETECTOR				
511	62.4 ± 3	17.47 ± 6	427.0 ± 6	88 ± 3
1275	142 ± 5	43.60 ± 6	522.0 ± 6	88 ± 3

Table 1: Signal output from scintillators

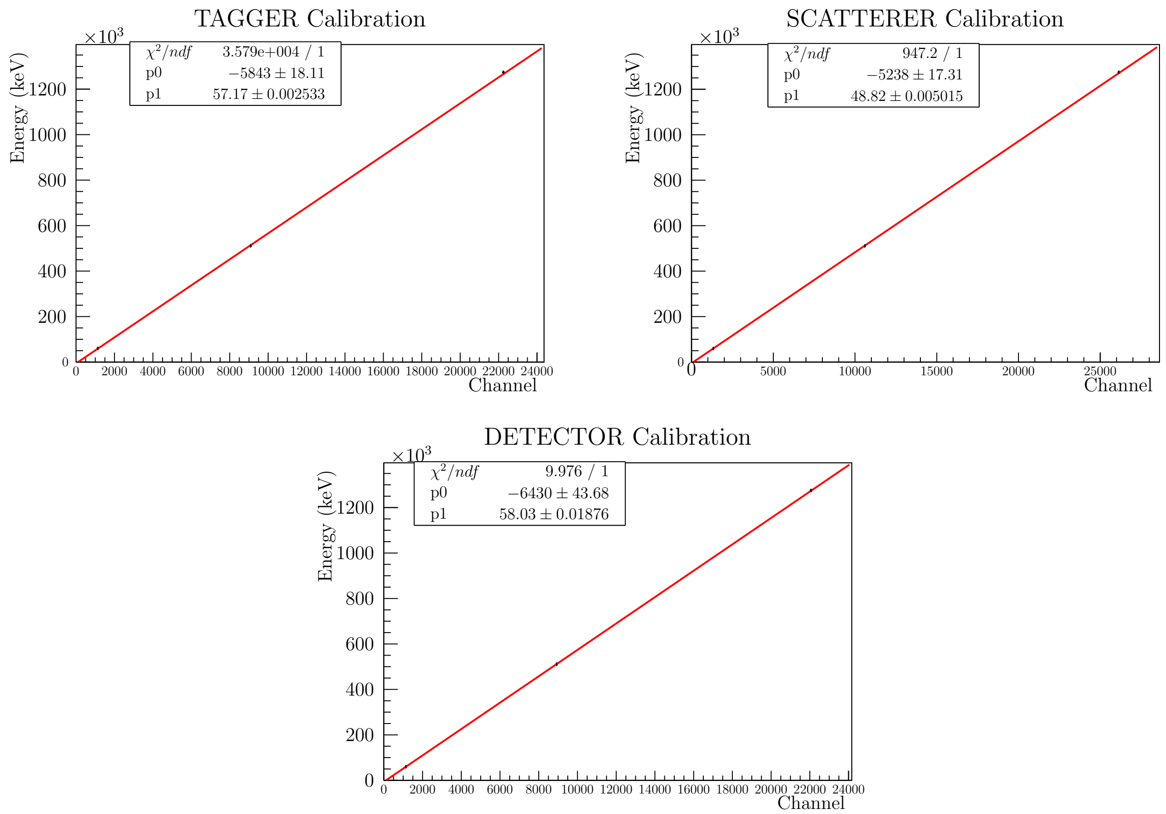

Figure 1: Calibration fit (in order TAGGER, SCATTERER, DETECTOR)

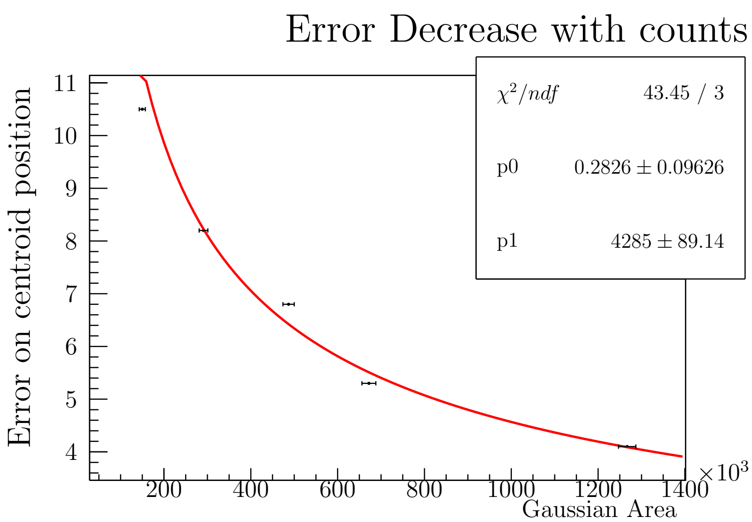

Figure 2: Position error in function of peak area

delayed output signals was created by changing the widths of the three delayed signals (in this measurements the DETECTOR was at an angle $\theta = 90°$). The values of widths of the three signals are reported in Tab. 2.

Detector	CFTD Delayed signal Width (ns)	Counting rate (counts/s)
TAGGER	114 ± 5	3180 ± 44
SCATTERER	110 ± 5	3450 ± 60
DETECTOR	108 ± 5	605 ± 26

Table 2: Widths of the delayed signals and counting rate of the detectors.

With the use of Tektronik oscilloscope and the microswitches of the CFTD delays, firstly it was obtained an overlap between SCATTERER and TAGGER and then with a second Na-22 source placed between DETECTOR and TAGGER another coincidence between these signals was obtained. Having checked the presence of overlapping regions, the CFTD delayed outputs were connected to Logic Unit inputs 1,2,3 with FOLD=3 in order to obtain the trigger for the data acquisition. After having defined the measurement geometry, fixing the distances D1 source-TAGGER, D2 source-SCATTERER, D3 SCATTERER-DETECTOR:

D1=(3.5±1)cm
D2=(8.5±1)cm
D3=(19.5±1)cm

it was possible to estimate the counting rates from the known activity of the Na-22 source, A = 60.1 kBq, considering that the collimator allows to have a collimated beam with diameter $\Phi <$ 3.5cm and calculating the fraction of solid angle from the source to the TAGGER, $\frac{\Delta\Omega}{4\pi}$. The intensity of the 511 keV emitted gamma ray add a factor 1.8, obtained from the *nddc.bnl.gov* database and the efficieny of the NaI(Tl) detector was supposed to be $eff \simeq= 0.5$

$$C_{rate}^{TAG} = 1.8 \cdot A \cdot \frac{\Delta\Omega}{4\pi} \cdot 0.5$$

For the presence of the collimator, all the beam arrives to the SCATTERER and the expected counting rate can be estimated to be similar to the one of the TAGGER: $C_{rate}^{SCAT} \simeq C_{rate}^{TAG}$ For the case of the DETECTOR it is necessary to consider the diameter of the detector, which was measured to be ($d = 7.5 \pm 0.1$) cm, in order to take into account only the right fraction of angle in the estimate of the counting rate:

$$C_{rate}^{DET} = 1.8 \cdot A \cdot \frac{\Delta\Omega}{4\pi} \cdot \frac{\Delta\theta}{2\pi}$$

The estimated counting rates are reported in Tab.3.

Detector	Estimated counting rate (counts/s)
TAGGER	3380
SCATTERER	3380
DETECTOR	83

Table 3: Estimated counting rates with the defined measurement geometry.

In the case of the DETECTOR this estimated values are lower than the ones measured previously, as in this case only the events related to the photons emitted at 511 keV were considered, while in the acquisition all possible events were detected.

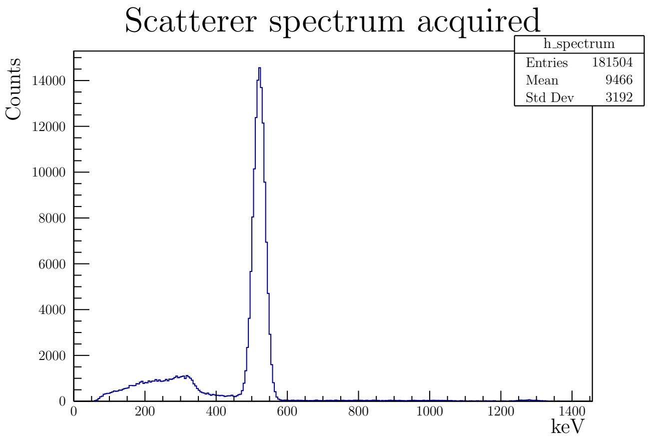

Figure 3: SCATTERER spectrum acquired considering only the coincidences TAGGER-SCATTERER

Angle	Measured counting rate (counts/s)	Angle	Measured counting rate (counts/s)
10 degrees		**60 degrees**	
TAGGER	3766	TAGGER	3812
SCATTERER	3104	SCATTERER	2915
DETECTOR	915	DETECTOR	625
TRIGGER	9	TRIGGER	4
40 degrees		**90 degrees**	
TAGGER	3786	TAGGER	3730
SCATTERER	3070	SCATTERER	2992
DETECTOR	751	DETECTOR	550
TRIGGER	5	TRIGGER	3

Table 4: Counting rates measured at different angles.

After having disconnected the DETECTOR from the Logic Unit and having selected FOLD=2, it was possible to acquire a spectrum of the SCATTERER, considering only the coincidences between the SCATTERER and TAGGER for the trigger in the data acquisition. This spectrum is reported in Fig.3.

Using the coincidences between TAGGER and SCATTERER to trigger the data aquisition we observe a peak near 511 keV for the SCATTERER as in this configuration we are selecting only the events related to the two 511 keV photons which are emitted by the Na-22 source as they are emitted back to back, while for the case of 511-1275 keV coincidences, for each of the 511 keV identified by the TAGGER the 1275 keV photon correlated can be emitted isotropically.

After having analyzed the coincidences between TAGGER ans SCATTERER, the delayed output of the DETECTOR CFTD was inserted in the Logic Unit and FOLD=3 was selected in order to acquire the spectrum of the three detectors in coincidence and to evaluate the energy of the scattered photon and electron at different angles. Firstly for each angular position selected for the DETECTOR the counting rate of each signal and of the trigger was measured, reported in Tab.4.

From the measured counting rates it would have been possible to decide for every angle of acquisition the proper measurement time, in this case however due to the problem in the connection of the digitizer during the first day of the experience, the acquisition time was limited to what was strictly necessary and only 4 angular position were considered in the measurements (10°, 40°, 60°, 90°), choosing a time of 20 minutes for the first two cases and 25 minutes for 60 degrees. At 90 degrees the measurement was taken during the night between the second and the third day. As an example of the acquired spectra, in Fig.4 the ones obtained for the 90 degrees configuration are shown, after having been calibrated.

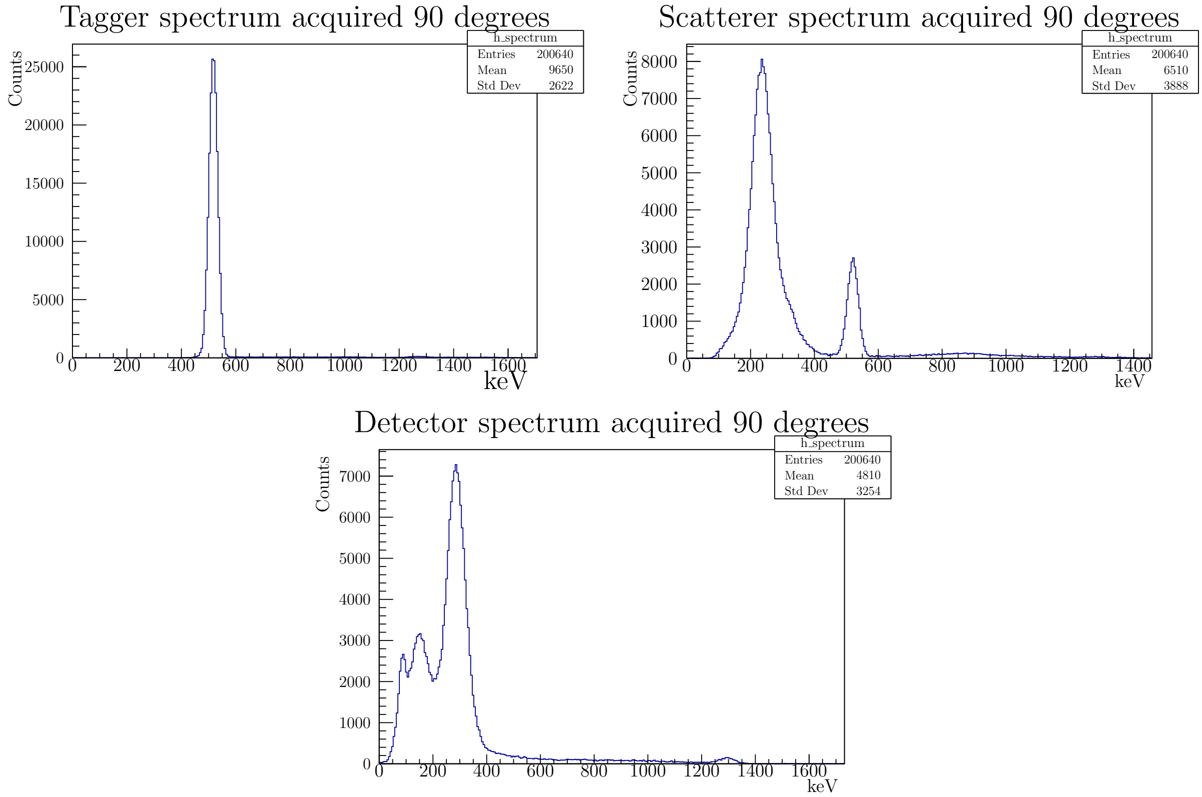

Figure 4: Spectra acquired with the DETECTOR at 90 degrees (In order TAGGER, SCATTERER, DETECTOR).

As it may be seen directly from the acquired spectra, the use of the three coincidences allowed to select for the TAGGER only the 511 keV emitted photons, while in the spectrum of the SCATTERER there is an evident peak near 250 keV represented by the scattered electrons and a second peak for the 511 keV emitted photons. In the case of the DETECTOR it is present a peak around 250 keV for the detected scattered photons, with a clear Compton edge just before.

To determine the energy of the scattered photon and of the scattered electron in the different angular positions a MACRO for ROOT was used, which selected only the events in the three spectra which verify the conditions to be close to the full energy peak of the 511 keV photon in the TAGGER spectrum (between 468.7 keV and 577.5 keV) and close to the full energy peak of the scattered electron in the SCATTERER spectrum (15.0keV-102.9keV for 10°, 43.6keV-189.9keV for 40°, 92.4keV-214.4keV for 60°, 189.9keV-287.6keV for 90°): the coincidence of these two conditions defined the number of diffused photon for each angular position. For the new spectra obtained by the events selected in this way, the peaks in the SCATTERER and in the DETECTOR were fitted with a gaussian in order to determine the energies of the scattered electron and photon. An example of the spectra obtained by the condition to select the events is shown in Fig.5. In order to determine the diffused events for each angle it was considered the integral under the scattered photon peak in the DETECTOR spectra, removing the background events with a linear fit around the peak so that the number of events not related to the scattered photon could be estimated by the area under the straight line over the region of the peak, as shown in Fig.6 in the case of 90 degrees.

In Tab.5 the DETECTOR angle, total number of diffused events, average photon energy revealed by the DETECTOR and average electron energy revealed by the SCATTERER are shown. As it may be seen in the last column of Tab.5 the sum of the revealed energies event by event gives a value which is greater than the 511 keV of the emitted photon, this effect may interpreted as a consequence

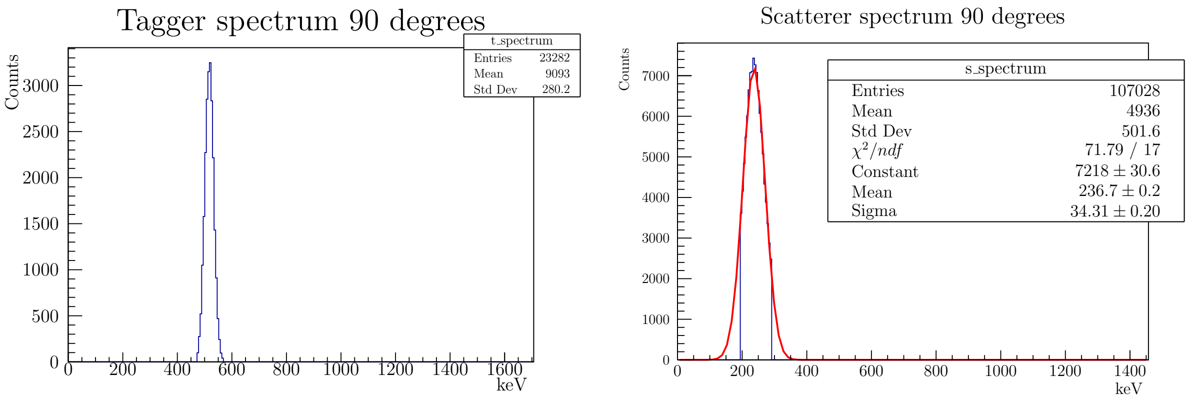

Figure 5: TAGGER and SCATTERER spectrum obtained from the data analysis with the DETECTOR at 90 degrees.

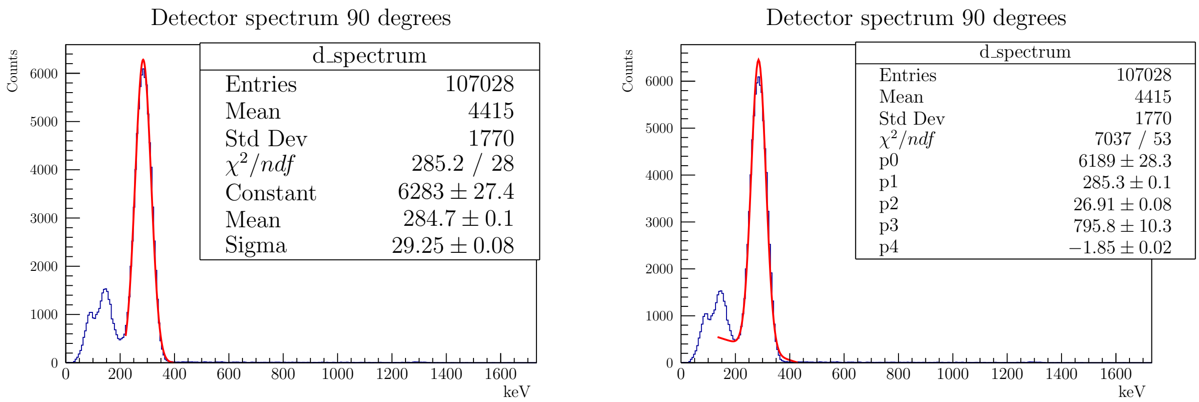

Figure 6: DETECTOR spectrum and Fit on the DETECTOR spectrum used for the analysis of the background events.

of the effective angle covered by the DETECTOR. As the theoretical cross section of Compton scattering and the energies of scattered photons are bigger for small angles, the contribution of photons with higher energies is predominant at lower angles and a shift to the right of the photon peaks is obtained, with a final overestimation of the total energy. This effect is weaker in the case of higher angles, as in this case cross section is lower and it varies slowly, so that the values obtained at 90 degrees is nearer to the theoretical prediction from energy conservation. In Tab.6 the values of the scattered photon and electron energies obtained selecting the events with energy conservation are shown. In this case it may be seen that the energies follow the same general trend as in the values reported in Tab.5, giving a proof of the energy conservation during the scattering process, as selecting the diffused events in this way it was obtained the same final result.

Angle	**Number of diffused events**	**Photon energy**	**Electron energy**	**Energies sum**
10 degrees	130	(421.1 ± 1.6)keV	(114.1 ± 2.5)keV	(535.2 ± 3.9)keV
40 degrees	424	(379.9 ± 1.5)keV	(158.9 ± 2.2)keV	(538.8 ± 3.7)keV
60 degrees	631	(359.5 ± 1.2)keV	(171.0 ± 1.8)keV	(530.5 ± 3.0)keV
90 degrees	77911	(284.7 ± 0.1)keV	(236.7 ± 0.2)keV	(521.4 ± 0.3)keV

Table 5: Energy of the scattered photon and electron and number of diffused events at different angles.

In Fig.7 there are the measured values of the energies of the scattered photons and electrons

Angle	**Photon energy**	**Electron energy**
10 degrees	(346 ± 2)keV	(183 ± 3)keV
40 degrees	(341 ± 2)keV	(176 ± 4)keV
60 degrees	(338 ± 2)keV	(176 ± 2)keV
90 degrees	(281.4 ± 0.2)keV	(234.2 ± 0.1)keV

Table 6: Energy of the scattered photon and electron with single event energy conservation.

and the theoretical predictions with $h\nu_i = 511$keV.

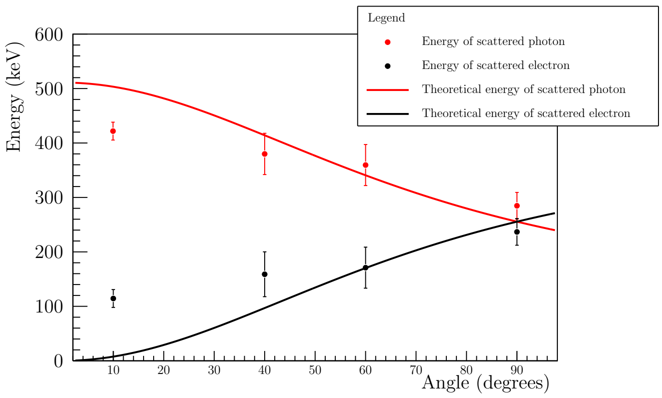

Figure 7: Comparison between the measured energies and the theoretical predictions.

It may be seen that the measured energies have a general trend reminiscent of the theoretical prediction, although for the lower angles there is an higher difference between the experimental data and the theoretical prediction, as it is evident for the energy at 10 degrees. This deviation is related with the strong dependence of the cross section for Compton scattering on the angle, especially for small ones. The experimental setup used to measure the energies gave an estimate of the angle of the DETECTOR with a finite acceptance, which can be taken into account if it is considered that the diameter of the DETECTOR was measured to be $d = (7.5 \pm 0.1)$cm and the distance SCATTERER-DETECTOR was given by $D3 = (19.5 \pm 1)$cm. The effective angle covered by the DETECTOR in the data acquisition is then given by the value:

$$\theta_{eff} = \frac{d}{D3} \cdot \frac{180^\circ}{\pi} = (22.03 \pm 0.02)^\circ$$

To take into account the effective angle covered by the DETECTOR for the errors on the energies in Fig.7 it was considered the difference between the value of the theoretical energy for 5.5 degrees more than the value given by the goniometer and the theoretical value 5.5 degrees below.

To show the correlation in the events detected by the SCATTERER and the DETECTOR in Fig.8, there are the bidimensional energy spectrum for the SCATTERER(x axis)-DETECTOR(y axis) in the 90 degrees configuration.

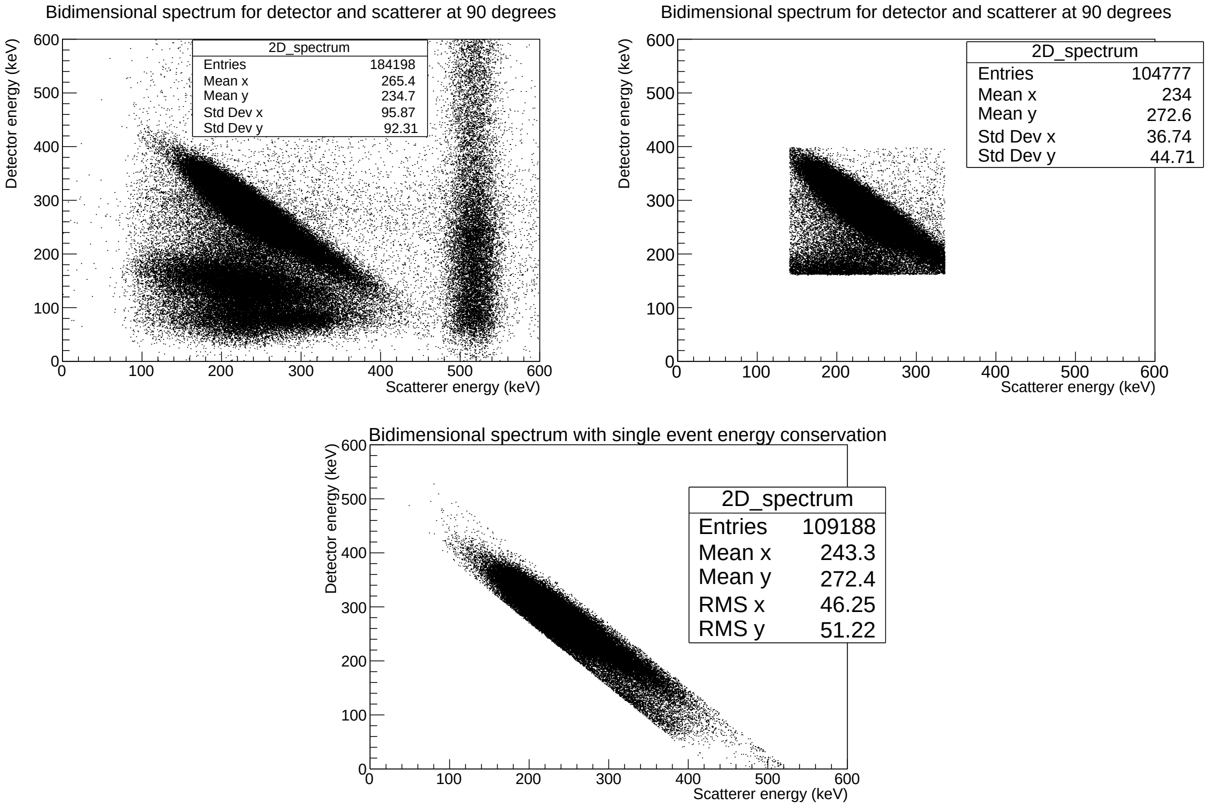

Figure 8: Bidimensional spectrum SCATTERER-DETECTOR, with filter centered on peaks and with single event energy conservation.

As it may be seen directly from the graphs, there is an evident correlation between the data acquired from SCATTERER and DETECTOR in the region of 250 keV and using the condition to select the acquired data only close to the full energy peaks this correlation is even more precise. In Fig.8, instead, the same graph with only events for which the sum of the energy is approximately 522 keV is shown, with the same evident correlation.

Measurement of the cross section

In order to verify the relation of the differential cross section in function of the angle of scattering θ, the SCATTERER detector was replaced by a cylindrical sample of aluminium (Al). The measured radius r and the thickness h are:

$$r = (1.5 \pm 0.1)cm \qquad h = (0.8 \pm 0.1)cm$$

and the volume V of the sample results $V = (5.65 \pm 0.08)cm^3$.

To estimate the experimental differential cross section at different angles θ_f it was used the following expression:

$$\left[\frac{d\sigma\left(\theta_f\right)}{d\Omega}\right]_{exp} = \frac{\Sigma_\gamma}{\left(\varepsilon \cdot N \cdot \Delta\Omega_f \cdot I/S\right)} \tag{2}$$

in which Σ_γ is the number of events in the full energy peak in the spectrum of the scattered photon revealed by the DETECTOR, ε is the photopic efficiency for the energy of scattered photons, N is the number of electrons in the sample of Al , $\Delta\Omega_f$ is the solid angle underlined by the DETECTOR and I/S is the number of photons accidental on the sample per unit of surface.

In order to measure the photopic efficiency of the 511 keV photon peak, the aluminium sample was dismounted and the DETECTOR was placed at 0 degrees in contact with the exit of the lead collimator, just to ensure all the tagged beam was in its angular acceptance. Selecting for the trigger signal in data acquisition the coincidence between TAGGER and DETECTOR the two spectrum reported in Fig.9 were acquired.

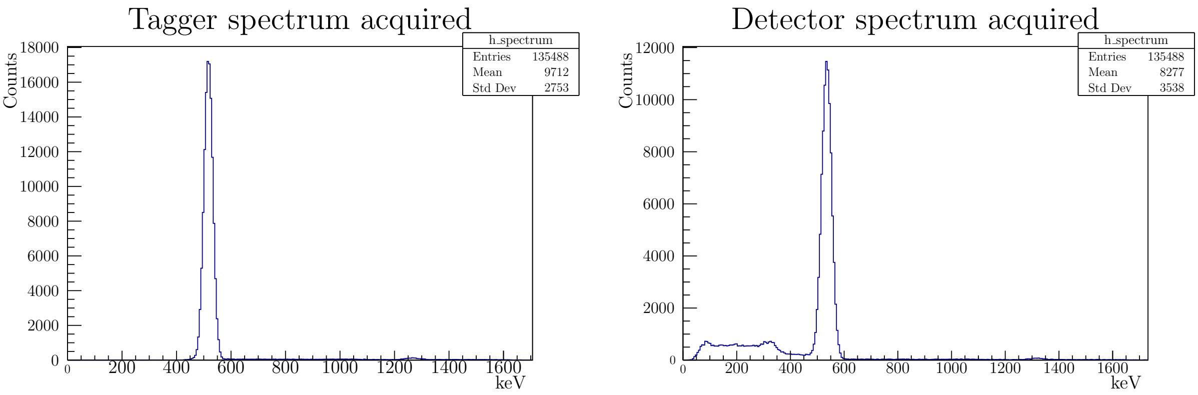

Figure 9: Spectra acquired to estimate the efficiency ε (In Order TAGGER and DETECTOR).

From this two gamma spectra it was possible to calculate the total number of events (N_{tot}), integrating under the 511 peak in the TAGGER spectrum, and the number of scattering events (N_1), integrating under the peak in DETECTOR spectrum, subtracting the background effects related to the Compton edge of the 1275 keV scattered photon. The obtained values were:

$N_{tot} = (135.5 \pm 0.4) * 10^3 \qquad N_1 = N - N_{background} = (92.5 \pm 0.3) * 10^3 - (13.2 \pm 0.1) * 10^3 = (79.3 \pm 0.3) * 10^3$

Assuming that for each photon recorded in the TAGGER there was a photon recorded in the DETECTOR, for the spatial correlation of the system, the full-energy efficiency ε at the 511 keV peak of the DETECTOR is given by:

$$\varepsilon(511keV) = \frac{N_1}{N_{tot}} = (58.5 \pm 0.4)\%.$$

To measure the number of events in the full energy peak (Σ_γ), the spectrum of events detected by the DETECTOR was acquired at different angles: 30°, 60°, 90°. From the total number of events due to $511keV$ photons, the background due to the Compton shoulder of the $1275keV$ photons was subtracted. During the measurement, the total number of events in the TAGGER (N_{scaler}) was recorded and the number I of 511keV photons that hit the aluminium sample and deposited 511keV in the TAGGER was measured by the following:

$$I = N_{scaler} \cdot F(511)$$

where F(511) previously obtained is equal to 0.4891 ± 0.0007.

In Tab.7 the recorded values of N_{scaler} and the measured values of Σ_γ and I are reported. Errors were measured using the error propagation formula.

The number of electrons in the sample $N = (4,4 \pm 0.5) * 10^{24}$ was given by the relation $N = \frac{V \times density \times N_{Avogadro} \times Z_{Al}}{M_{atomic}}$, where $density = 2.7g/cm^3$, $Z_{Al} = 13$, $M_{atomic} = 26.98\frac{g}{mol}$.

The solid angle underlined by the DETECTOR was measure as $\Delta\Omega_f = \frac{\pi r^2}{d^2}$, where $r = (3.75 \pm 0.05)$cm is the radius of the detector while $d = (14 \pm 1)$cm is the distance between the DETECTOR and the aluminium sample.

The theoretical differential cross section was obtained by the following equation:

$$\left[\frac{d\sigma}{d\Omega}\right]_{th} = \frac{r_e^2}{2}\left(\frac{h\nu_f}{h\nu_i}\right)^2\left(\frac{h\nu_f}{h\nu_i} + \frac{h\nu_i}{h\nu_f} - sin(\theta)^2\right) \tag{3}$$

Angle	$\Sigma_\gamma * 10^3$	$N_{scaler} * 10^3$	$I * 10^3$
30°	(43.1 ± 0.2)	(1541 ± 1)	(753.5 ± 0.6)
60°	(5.42 ± 0.09)	(1996 ± 1)	(975.8 ± 0.7)
90°	(3.41 ± 0.07)	(2442 ± 2)	(1194.1 ± 0.8)

Table 7: Number of events in the full energy peak in the spectrum of scattered photons (Σ_γ), total number of events in the TAGGER (N_{scaler}), number of photons that hit the Aluminium sample and deposited 511 keV in the TAGGER I.

in which $r_e = e^2/m_ec^2$ is the classical radius of the electron, $h\nu_i$ and $h\nu_f$ are the energies of the incident and diffused photon and θ is the scattering angle.

The energy of the diffused photon was measured by Eq.4:

$$h\nu_f = \frac{h\nu_i}{1 + \frac{h\nu_i}{m_ec^2}(1 - cos\theta)} \tag{4}$$

In Tab.8 the experimental and theoretical differential cross sections at 30°, 60°, 90° are reported.

Angle	$[\frac{d\sigma}{d\Omega}]_{exp}(cm)^2$	$[\frac{d\sigma}{d\Omega}]_{th}(cm)^2$
30°	$(7 \pm 1)10^{-25}$	$(5 \pm 1)10^{-26}$
60°	$(7 \pm 1)10^{-26}$	$(3.9 \pm 0.8)10^{-26}$
90°	$(3.5 \pm 0.6)10^{-26}$	$(3.1 \pm 0.6)10^{-26}$

Table 8: Experimental and theoretical differential cross sections at different angles.

In the case of 30 degrees, the difference of one order of magnitude between the experimental estimate of the cross section and the theoretical value can be explained considering the effective extension of the angle covered by the detector θ_{eff}, given by:

$$\theta_{eff} = \frac{2r}{d}\frac{180°}{\pi} = (31 \pm 2)°$$

As the cross section is strongly variable for small angles the value obtained experimentally for the 30 degrees given by the goniometer is not compatible with the theoretical one.

Fig.10 shows the background spectrum acquired for a night. The background results negligible in respect to the signal events used in the analysis.

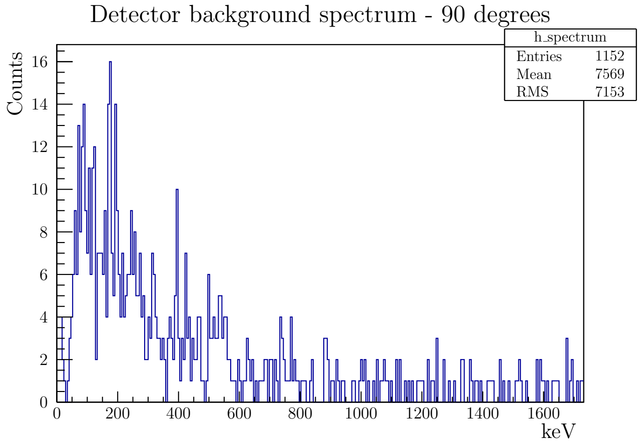

Figure 10: Background spectrum acquired by the DETECTOR at 90 degrees.

Conclusion

During the laboratory experience the energy distribution and the Compton scattering cross section were measured for various angles using NaI(Tl) detectors. The energy distribution follows the trend of the theoretical predictions but for small angles there is an overestimation of the electron energy and an underestimation of the photon energy, however the sum of the energies is conserved in the process. The measured cross section values are within one order of magnitude of the theoretical predictions. Due to the problem with the digitizer the number of measurements and their duration had to be reduced, however it was still possible to show how the quantities follow the expected behaviour.